Wave Optics in Black Hole Spacetimes: Schwarzschild Case

Yasusada Nambu[1] **and Sousuke Noda**[2]

E-mail: [1] nambu@gravity.phys.nagoya-u.ac.jp

E-mail: [2] noda@gravity.phys.nagoya-u.ac.jp
Department of Physics, Graduate School of Science, Nagoya University, Chikusa, Nagoya 464-8602, Japan

Abstract. We investigate the wave optics in the Schwarzschild spacetime. Applying the standard formalism of wave scattering problems, the Green function represented by the sum over the partial waves is evaluated using the Poisson sum formula. The effect of orbiting scattering due to the unstable circular orbit for null rays is taken into account as the contribution of the Regge poles of the scattering matrix and the asymptotic form of the scattering wave is obtained in the eikonal limit. Using this wave function, images of the black hole illuminated by a point source are reconstructed. We also discuss the wave effect in the frequency domain caused by the interference between the direct rays and the winding rays.

PACS numbers: 04.20.-q, 04.70.-s, 42.25.Fx

Submitted to: *Class. Quantum Grav.*
Keywords: wave optics, image formation, black hole, wave scattering

1. Introduction

Physics of wave propagation and wave excitation in black hole spacetimes has been investigated as a tool to comprehend properties of black hole spacetimes. Especially, the quasi-normal mode of black holes is directly related to the structure of black hole spacetimes and is expected to be confirmed observationally in near future using gravitational waves. In the high frequency eikonal limit, the quasi-normal mode is connected to the wave scattering in the vicinity of the peak of the effective potential and thus related to the existence of the unstable circular orbit for null rays around the black hole. The geometric interpretation of the quasi-normal frequency is as follows; its real part corresponds to the period for a massless particle or null rays in the unstable circular orbit and its imaginary part represents the decay rate from the unstable circular orbit [1, 2, 3, 4].

On the other hand, also related to the existence of the unstable circular orbit, properties of "shadows" of black holes [5, 6, 7] have been studied in detail recently. The main motivation of this subject is direct verification of black hole spacetimes using VLBI radio telescopes. The shadow of the black hole is defined as the region of absorption on the observer's screen and its rim corresponds to the unstable circular orbit of null rays around the black hole projected on the observer's screen. Its shape can be drawn by integrating null geodesics in the black hole spacetime (ray tracing). Recently, we have investigated the imaging of black holes using waves [8, 9]; instead of applying the ray tracing method, the image of the black hole is obtained using the Fourier transformation of the scattering wave at the observer. In this method, wave effects such as interference can be included in images of black hole shadows.

Wave optical treatment of the gravitational lensing has already done and detectability of the interference effect is discussed for the weak gravitational lensing [10, 11, 12, 13]. For ordinal astrophysical sources, we cannot expect to observe the spatial interference fringe pattern because the coherent time of the source is too short compared to the path difference in the gravitational lensing system. However, even for such a case, the interference effect can be observable in the frequency domain as the oscillation of the power spectrum. The period of the oscillation in the power spectrum is determined by the mass of the gravitational source which gives rise to the gravitational lensing [14]. For the gravitational lensing by the black hole, a new interference effect associated with the existence of the unstable photon orbit is expected; null rays can go around the black hole arbitrary number of times (orbiting) and direct rays and these winding rays can interfere and the beat appears in the power spectrum. We expect that the period of the beat is related to the mass of the black hole and the radius of the unstable circular orbit.

In this paper, we consider wave optics in the Schwarzschild spacetime using a massless scalar field to investigate wave effects peculiar to black hole spacetimes. The massless scalar field is adopted as the benchmark treatment for the wave scattering problem by black holes and we do not consider polarization degrees of freedom which

is necessary for the electro magnetic waves and gravitational waves. We follow the standard treatment of the wave scattering problem by black holes [15, 16, 19] and derive the asymptotic form of the scattered wave at sufficiently far from the black hole in the high frequency eikonal limit. The wave is represented by the sum over the partial waves which include the WKB phase shift. Comparing to the standard treatment of the wave scattering theory, our formulation retains the next to leading order contribution in the phase of the scattering wave at large r, and this refinement makes the sum over partial waves converge even for the scattering caused by the long range $1/r$ potential.

We shows that the gravitational lens equation in the black hole spacetime can be derived by taking the short wavelength limit of the scattering wave. This lens equation is an extension of the relation between the scattering angle and the derivative of the WKB phase shift which is derived by the stationary phase method [20, 21]. To evaluate the sum over partial waves, we apply the complex angular momentum (CAM) method [22, 23, 17, 18, 19]. The scattering wave is decomposed to the direct part and the winding part. The winding part can be evaluated using Regge poles which are associated with the existence of the unstable circular orbit around the black hole.

The outline of this paper is as follows. In Sec. II, we introduce the WKB Green function and derive the lens equation from the Green function by the stationary phase method. In Sec. III, we shortly review the S-matrix and the Regge poles. We evaluate the sum over partial waves and obtain the asymptotic form of the scattering wave in Sec. IV. As applications, we consider images of the black hole and the interference effect in the power spectrum in Sec. V. Sec. VI is devoted to summary. We use units in which $c = \hbar = G = 1$ throughout this paper.

2. Wave scattering by a black hole

We investigate the wave scattering problem by the black hole in the high frequency eikonal limit. The high frequency condition is $M\omega \gg 1$ where M is the mass of a black hole. Thus this condition states that the wave length is sufficiently shorter than the size of the black hole. The eikonal limit is the angular quantum number ℓ of the wave is larger than unity $\ell \gg 1$. Under these conditions, we follow the standard approach of the wave scattering theory; decompose scattered waves to the sum over partial waves and introduce the phase shift which represents the properties of the scatterer.

2.1. Wave equation and the WKB phase shift

Let us consider the scalar wave equation $\Box\Phi = 0$ in the Schwarzschild spacetime. The metric is

$$ds^2 = -\left(1 - \frac{2M}{r}\right) dt^2 + \left(1 - \frac{2M}{r}\right)^{-1} dr^2 + r^2 d\Omega^2. \tag{1}$$

As the geometry has the spherical symmetry, for the wave configuration with axial symmetry about the z-axis, the scalar field Φ is separable as

$$\Phi = e^{-i\omega t} R_\ell(r) P_\ell(\cos\theta). \tag{2}$$

The radial wave function R_ℓ and the angular wave function P_ℓ satisfy

$$\frac{d}{dr}\left(\Delta \frac{dR_\ell}{dr}\right) + \left(\frac{r^4\omega^2}{\Delta} - \ell(\ell+1)\right) R_\ell = 0, \tag{3}$$

$$\frac{1}{\sin\theta}\frac{d}{d\theta}\left(\sin\theta \frac{dP_\ell}{d\theta}\right) + \ell(\ell+1) P_\ell = 0, \tag{4}$$

where $\Delta = r^2 - 2Mr$. We consider the WKB solution of the radial equation with the assumption of the high frequency eikonal limit $M\omega \gg 1$, $\ell \gg 1$. By introducing a new radial function $\psi_\ell = rR_\ell$ and the tortoise coordinate $r_* = \int dr \frac{r^2}{\Delta} = r + 2M\ln(r/(2M) - 1)$, the radial equation becomes

$$\frac{d^2\psi_\ell}{dr_*^2} + Q\psi_\ell = 0, \tag{5}$$

$$Q = \omega^2 - \left(\frac{\ell(\ell+1)}{r^2} + \frac{2M}{r^3}\right)\left(1 - \frac{2M}{r}\right).$$

The lowest order WKB solution of this equation is

$$\psi_\ell = Q^{-1/4} \exp\left[i\int^{r_*} dr_*\, Q^{1/2}\right] \propto e^{iS_r}. \tag{6}$$

For the angular wave function, which is the Legendre function in the present case, it also can be written in the WKB form $P_\ell \propto e^{iS_\theta}$. For $\ell, M\omega \gg 1$, the phase functions S_r and S_θ satisfy the following Hamilton-Jacobi equations

$$\left(\frac{dS_r}{dr}\right)^2 - \frac{1}{\Delta^2}\left(r^4\omega^2 - \ell(\ell+1)\Delta\right) = 0, \tag{7}$$

$$\left(\frac{dS_\theta}{d\theta}\right)^2 - \ell(\ell+1) = 0. \tag{8}$$

These equations are the same as the Hamilton-Jacobi equations for null rays in the Schwarzschild spacetime. The solutions of these equations are

$$S_r(r) = \int^r dr \frac{\sqrt{\mathcal{R}}}{\Delta}, \quad S_\theta(\theta) = \int^\theta d\theta\, L = L\,\theta, \tag{9}$$

where $\mathcal{R}(r) = \omega^2 r^4 - L^2\Delta$ and we have replaced $\ell(\ell+1)$ by $L^2 \equiv (\ell + 1/2)^2$, which improves the accuracy of the WKB approximation; this replacement ensures the phase shift introduced in (16) zero for the flat limit $M = 0$. Following the standard Hamilton-Jacobi theory, by differentiating the function $S_r + S_\theta$ with respect to the angular momentum L, the equation for the trajectory of null rays is derived as

$$-L\int_{r_i}^{r_f} \frac{dr}{\sqrt{\mathcal{R}}} = -(\theta_f - \theta_i). \tag{10}$$

From this equation, the deflection angle for null rays is obtained by taking $r_i, r_f \to \infty$:

$$\Theta = \pi - (\theta_f - \theta_i) = \pi - 2L\int_{r_0}^{\infty} \frac{dr}{\sqrt{\mathcal{R}}}, \tag{11}$$

where r_0 is the radial turning point determined by $\mathcal{R}(r_0) = 0$.

We rewrite the WKB radial function using the phase shift. For this purpose, we consider the solution of the radial equation (5) with the following boundary condition:

$$u_{\rm in} \sim \begin{cases} e^{-i\omega r_*}, & r_* \to -\infty, \\ A_{\rm out}\, e^{i\omega r_*} + A_{\rm in}\, e^{-i\omega r_*}, & r_* \to +\infty. \end{cases} \tag{12}$$

The phase shift is defined by

$$e^{2i\delta_\ell} = -(-)^\ell \frac{A_{\rm out}}{A_{\rm in}}. \tag{13}$$

Then the wave at $r \to +\infty$ is expressed as

$$\begin{aligned} u_{\rm in} &\sim A_{\rm out}\, e^{i\omega r_*} + A_{\rm in}\, e^{-i\omega r_*} \\ &\propto \sin\left(\omega r_* + \delta_\ell - \frac{\pi\ell}{2}\right). \end{aligned} \tag{14}$$

For $\delta_\ell = 0$, $u_{\rm in}$ corresponds to the spherical wave in the flat spacetime $j_\ell(\omega r) \sim \sin(\omega r - \pi\ell/2)$. Within the WKB approximation, the analytic continuation around the turning point yields the radial function for large r as

$$\begin{aligned} u_{\rm in}(r) &\approx \sin\left[\int_{r_{\rm t}}^{r_*} dr_*\, Q^{1/2} + \frac{\pi}{4}\right] \\ &= \sin\left[\omega r_* + \delta_\ell - \frac{\pi\ell}{2} - \int_r^\infty dr \frac{r^2}{\Delta}\left(Q^{1/2} - \omega\right)\right], \end{aligned} \tag{15}$$

where $r_{\rm t}$ is the turning point determined by $Q(r_{\rm t}) = 0$. Hence the WKB phase shift in the Schwarzschild spacetime is obtained as [16]

$$\delta_\ell = \int_{r_{\rm t}}^\infty dr \frac{r^2}{\Delta}\left(Q^{1/2} - \omega\right) - \omega r_{{\rm t}*} + \frac{\pi}{2}\left(\ell + \frac{1}{2}\right). \tag{16}$$

For small ℓ less than a some critical value ℓ_c, there exists no real solution for $Q(r) = 0$ and (16) has no meaning. However, by performing a suitable analytic extension of the formula, it can be shown that the phase shift acquires an imaginary part which represents the absorption of waves by the black hole. In the eikonal limit $\ell \gg 1$, $Q(r) \approx \mathcal{R}(r)/r^4$ and the phase shift is

$$\delta_\ell = \int_{r_0}^\infty dr \left(\frac{\sqrt{\mathcal{R}}}{\Delta} - \frac{r^2}{\Delta}\omega\right) - \omega r_{0*} + \frac{\pi}{2}\left(\ell + \frac{1}{2}\right), \tag{17}$$

and by differentiating with respect to the angular momentum ℓ,

$$\frac{d\delta_\ell}{d\ell} \approx \frac{\pi}{2} - \left(\ell + \frac{1}{2}\right)\int_{r_0}^\infty \frac{dr}{\sqrt{\mathcal{R}}}. \tag{18}$$

Comparing to Eq. (11), we thus obtain the well known relation between the classical deflection angle and the WKB phase shift [22]

$$\Theta = 2\frac{d\delta_\ell}{d\ell}. \tag{19}$$

For large r, the integral in the phase of the radial wave function (15) can be approximated to be

$$-\int_r^\infty dr\left(1+\frac{2M}{r}\right)\left(Q^{1/2}-\omega\right)\approx\int_r^\infty dr\frac{(\ell+1/2)^2}{2\omega r^2}=-\frac{(\ell+1/2)^2}{2\omega r}, \quad (20)$$

where we assume that the function $Q^{1/2}$ is real so ℓ must satisfies $\sqrt{2}\,\omega r\geq\ell+1/2$ to make this approximation have meaning. This imposes the maximal upper limit $\ell_{\rm max}\approx\sqrt{2}\,\omega r$ for a fixed value of ωr when we take the partial wave sum.

In the standard formulation of the wave scattering problem, this term is treated as zero because it vanishes as $r\to\infty$ and does not contribute to the scattering amplitude and the differential cross section. However, as we will see, this term is necessary to reproduce the lens equation from the wave function in the eikonal limit and also necessary for convergence of the sum over partial waves.

After all, for sufficiently large r, we obtain the following form of the radial function in the eikonal limit

$$u_{\rm in}(r)\propto\sin\left[\omega r_*+\frac{(\ell+1/2)^2}{2\omega r}+\delta_\ell-\frac{\pi\ell}{2}\right]\quad\text{with}\quad\ell\leq\sqrt{2}\,\omega r. \quad (21)$$

2.2. Green function

We aim to obtain the scattered wave by a black hole; the scalar wave is emitted from a point source and scattered by the Schwarzschild black hole (see Fig. 1). For this purpose, let us consider the Green function for the scalar wave.

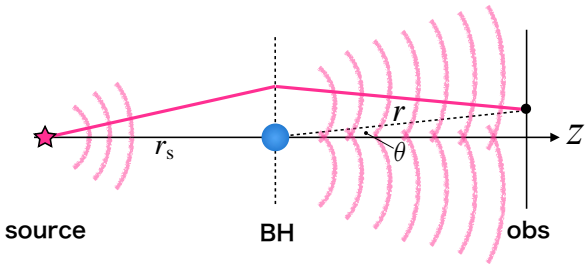

Figure 1. Configuration of wave scattering by a black hole.

For a monochromatic stationary wave with time dependence $e^{-i\omega t}$, the Green function satisfies

$$-g^{00}\omega^2\Phi+\frac{1}{\sqrt{-g}}\partial_j(\sqrt{-g}g^{jk}\partial_k\Phi)=-\delta^3(x,x_s). \quad (22)$$

where $\delta^3(x,x_s)$ denotes the invariant delta function $\frac{1}{\sqrt{-g}}\delta^3(x-x_s)$. By separating the wave function as

$$\Phi(r,\theta;r_s,\theta_s)=\sum_{\ell=0}^\infty\frac{2\ell+1}{4\pi r r_s}\psi_\ell(r,r_s)P_\ell(\cos\theta)P_\ell(\cos\theta_s), \quad (23)$$

the radial Green function $\psi_\ell(r, r_s)$ obeys‡

$$\frac{d^2\psi_\ell}{dr_*^2} + Q(r)\psi_\ell = -\delta(r_* - r_{s*}). \tag{24}$$

The solution of this equation can be constructed from a pair of linearly independent solutions of the radial equation; one is given by $u_{\rm in}$ in (12) and the other has the following asymptotic behavior

$$u_{\rm up} \sim \begin{cases} B_{\rm in}\, e^{-i\omega r_*} + B_{\rm out}\, e^{i\omega r_*}, & r_* \to -\infty, \\ e^{i\omega r_*}, & r_* \to +\infty. \end{cases} \tag{25}$$

Using these two independent solutions $u_{\rm in}, u_{\rm up}$, the radial Green function can be written as

$$\psi_\ell(r, r_s) = -\frac{u_{\rm in}(r_<)\, u_{\rm up}(r_>)}{W}, \tag{26}$$

where $r_> = \max(r, r_s), r_< = \min(r, r_s)$ and the Wronskian W is

$$W = u_{\rm in}\frac{du_{\rm up}}{dr_*} - u_{\rm up}\frac{du_{\rm in}}{dr_*} = 2i\omega A_{\rm in}. \tag{27}$$

For large r, r_s with $r_s < r$, the radial Green function is

$$\psi_\ell(r, r_s) \approx \frac{i}{2\omega} e^{i\omega r_*}\left(e^{-i\omega r_{s*}} - (-)^\ell e^{2i\delta_\ell}\, e^{i\omega r_{s*}}\right). \tag{28}$$

Assuming that the point source of the wave is located on $-z$ axis ($\theta_s = \pi$), the full Green function for the scattering problem is

$$\Phi(r, \theta; r_s, \theta_s) = \frac{i\omega}{4\pi r r_s}\sum_{\ell=0}^{\infty}(2\ell+1)(-)^\ell \psi_\ell(r, r_s) P_\ell(\cos\theta). \tag{29}$$

For $M = 0$ (free propagating wave in the flat spacetime), $\psi_\ell(r, r_s) = r r_s j_\ell(\omega r_s) h^{(1)}(\omega r)$ and this formula reduces to the Green function of the freely propagating wave in the flat spacetime:

$$\Phi_0 = \frac{i\omega}{4\pi}\sum_{\ell=0}^{\infty}(2\ell+1)(-)^\ell j_\ell(\omega r_s) h_\ell^{(1)}(\omega r) P_\ell(\cos\theta) = \frac{1}{4\pi}\frac{e^{i\omega|\mathbf{x}-\mathbf{x}_s|}}{|\mathbf{x}-\mathbf{x}_s|}. \tag{30}$$

Including the term $\frac{(\ell+1/2)^2}{2\omega r}$ in the phase of the radial function (28), the asymptotic form of the Green function at large r is

$$\begin{aligned}\Phi(r,\theta) &\approx \frac{e^{i\omega r_*}}{8i\pi\omega r r_s}\sum_{\ell=0}^{\infty}(2\ell+1)\left[e^{i\left(\omega r_{s*} + \frac{(\ell+1/2)^2}{2\omega}\left(\frac{1}{r}+\frac{1}{r_s}\right)+2\delta_\ell\right)} - (-)^\ell e^{-i\left(\omega r_{s*} + \frac{(\ell+1/2)^2}{2\omega}\left(-\frac{1}{r}+\frac{1}{r_s}\right)\right)}\right] P_\ell(\cos\theta) \\ &= \Phi_0 + \frac{e^{i\omega(r_{s*}+r_*)}}{4\pi r_s}\frac{1}{2i\omega r}\sum_{\ell=0}^{\infty}(2\ell+1)e^{i\frac{(\ell+1/2)^2}{2\omega\tilde{r}}}(e^{2i\delta_\ell}-1)P_\ell(\cos\theta),\end{aligned} \tag{31}$$

where $\Phi_0 \equiv \Phi|_{\delta=0}$ represents the incident spherical wave from the point source and we defined

$$\frac{1}{\tilde{r}} \equiv \frac{1}{r} + \frac{1}{r_s}. \tag{32}$$

‡ We use the relation $\sum_{\ell=0}^{\infty}(\ell+\frac{1}{2})P_\ell(\cos\theta)P_\ell(\cos\theta_s) = \delta(\cos\theta - \cos\theta_s)$.

Following the standard prescription of preparing the plane wave in the black hole spacetime [24], the spherical wave from the point source placed at sufficiently far from the black hole is obtained by replacing r, r_s in the phase factor of (30) to their tortoise coordinate r_*, r_{s*}:

$$\Phi_0 \approx \frac{e^{i\omega(r_{s*}+r_*)}}{4\pi(r+r_s)} e^{-i\omega\tilde{r}\frac{\theta^2}{2}} \quad \text{for} \quad \theta \ll 1 \text{ and large } r, r_s. \tag{33}$$

At this stage, we apply the Poisson sum formula§ to the sum in (31) which does not contain the phase shift:

$$\begin{aligned}
&\sum_{\ell=0}^{\infty}(2\ell+1)e^{i\frac{(\ell+1/2)^2}{2\omega\tilde{r}}}P_\ell(\cos\theta) \qquad (34)\\
&\quad = 2\sum_{m=-\infty}^{+\infty}\int_0^\infty d\lambda\,\lambda\, e^{i\frac{\lambda^2}{2\omega\tilde{r}}}P_{\lambda-1/2}(\cos\theta)\, e^{2im\pi(\lambda-1/2)}\\
&\quad \approx 2\int_0^\infty d\lambda\,\lambda\, e^{i\frac{\lambda^2}{2\omega\tilde{r}}}J_0(\lambda\theta) + 4\sum_{m=1}^{+\infty}\int_0^\infty d\lambda\,\lambda\, e^{i\frac{\lambda^2}{2\omega\tilde{r}}}J_0(\lambda\theta)\,\cos(2m\pi(\lambda-1/2))\\
&\quad = 2i\omega\frac{rr_s}{r+r_s}e^{-i\omega\tilde{r}\frac{\theta^2}{2}} + O((\omega\tilde{r})^0), \quad \text{for} \quad \theta \ll 1,
\end{aligned}$$

where we used the asymptotic formula for the Legendre function

$$P_{\lambda-1/2}(\cos\theta) \approx \left(\frac{\theta}{\sin\theta}\right)^{1/2} J_0(\lambda\theta) \quad \text{for} \quad \lambda \gg 1, \quad \theta \neq \pi, \tag{35}$$

and consider the scattering with small θ (forward direction) in the present analysis. We neglect $O(\omega^0)$ contribution which is higher order in the eikonal approximation. Therefore, for large r, the Green function in the form of the partial wave sum is

$$\begin{aligned}
\Phi &\approx \frac{e^{i\omega(r_*+r_{s*})}}{4\pi(r+r_s)}\left[e^{-i\omega\tilde{r}\frac{\theta^2}{2}} - e^{-i\omega\tilde{r}\frac{\theta^2}{2}} + \frac{r+r_s}{i\omega rr_s}\sum_\ell\left(\ell+\frac{1}{2}\right)e^{i\frac{(\ell+1/2)^2}{2\omega\tilde{r}}}\, e^{2i\delta_\ell}J_0((\ell+1/2)\,\theta)\right]\\
&= \frac{e^{i\omega(r_*+r_{s*})}}{4\pi i\omega rr_s}\sum_{\ell=0}^{\infty}\left(\ell+\frac{1}{2}\right)e^{i\frac{(\ell+1/2)^2}{2\omega\tilde{r}}}\, e^{2i\delta_\ell}J_0((\ell+1/2)\,\theta), \quad \text{for} \quad \theta \ll 1. \qquad (36)
\end{aligned}$$

In this formula, the factor $e^{i\frac{(\ell+1/2)^2}{2\omega\tilde{r}}}$ is essential to make the infinite sum over ℓ finite. Without this factor, the sum does not converge; this is well known property of the partial wave sum for long range potential which falls off as $1/r$ at large distances. We will discuss the issue of convergence of the partial wave sum (34) and (36) in the next subsection.

§ The Poisson sum formula is

$$\sum_{\ell=0}^{\infty}F(\ell+1/2) = \sum_{m=-\infty}^{+\infty}(-)^m\int_0^\infty F(\lambda)\, e^{i2\pi m\lambda}d\lambda.$$

We take a look at the scattering of the plane wave in the weak gravitational field of a point mass and check the formula (36) indeed works well. In this case, the deflection angle is given by the Einstein formula for light deflection

$$\Theta(b) = -\frac{4M}{b} \approx -\frac{4M\omega}{\ell}, \tag{37}$$

where $b = (\ell + 1/2)/\omega$ is the impact parameter for the partial wave. The phase shift is obtained by integrating the relation (19)

$$\delta_\ell = \frac{1}{2}\int^\ell d\ell\, \Theta(\ell) = -2M\omega \ln \ell + \text{const.} \tag{38}$$

By taking $r_s \to \infty$, the incident spherical wave reduces to the plane wave. Renormalizing the over all factor as $e^{i\omega r_{s*}}/(4\pi r_s) \to 1$ and applying the Poisson sum formula to (36),

$$\begin{aligned}
\Phi &= \frac{e^{i\omega r_*}}{i\omega r}\sum_{\ell=0}^{\infty}\left(\ell+\frac{1}{2}\right) e^{i\frac{(\ell+1/2)^2}{2\omega r}} e^{-i4M\omega\ln\ell} J_0((\ell+1/2)\theta) \qquad (39)\\
&= \frac{e^{i\omega r_*}}{i\omega r}\int_0^\infty d\lambda\,\lambda\, e^{i\frac{\lambda^2}{2\omega r}}\,\lambda^{-i4M\omega} J_0(\lambda\theta) + O(1/(\omega r))\\
&= e^{-i2M\omega\ln(4M\omega)}\, e^{i\omega r(1-\theta^2/2)}\, e^{\pi M\omega}\Gamma(1-i2M\omega)\,{}_1F_1\left(2iM\omega, 1, \frac{i}{2}r\omega\theta^2\right).
\end{aligned}$$

The phase factor $e^{-i2M\omega\ln(4M\omega)}$ can be absorbed to the constant of the phase shift. Then the obtained wave function has the following asymptotic form for $\omega r\theta^2 \gg 1$,

$$\Phi \approx e^{i\omega z - 2i\omega M\ln(\omega(r-z))} + M\frac{\Gamma(1-2iM\omega)}{\Gamma(1+2iM\omega)}\left(\frac{\theta}{2}\right)^{-2+4iM\omega}\frac{e^{i\omega(r+2M\ln(2\omega r))}}{r}, \tag{40}$$

where $z \approx r(1-\theta^2/2), r - z \approx r\theta^2/2$. The first term is the incident plane wave and the second term is the scattering wave. Thus (39) reproduces the scattering wave function for $1/r$ potential (Coulomb scattering). For $M\omega \gg 1, r\omega\theta^2 =$ finite, corresponding to the scattering toward the forward direction $\theta \sim 0$,

$$\Phi \approx e^{i\omega r(1-\theta^2/4)}\, e^{\pi M\omega}\,\Gamma(1-i2M\omega)\, J_0(\sqrt{4Mr}\,\omega\theta). \tag{41}$$

2.3. Convergence of partial wave sum

Here we comment on convergence of the partial wave sum (36). We truncate the infinite sum up to $\ell_{\max}$ and the phase shift is evaluated by the WKB formula (16). As we have mentioned in the last paragraph in Sec. 2.1, the upper bound of the partial wave sum in the eikonal approximation must be $\ell_{\max} = \sqrt{2}\,\omega r$, and this value becomes infinity in the eikonal limit. To check the convergence of this sum, we first consider (34) which is $\delta_\ell = 0$ case of (36). Let us consider the following quantity:

$$I(\theta, \ell_{\max}) = \frac{1}{2\omega r}\sum_{\ell=0}^{\ell_{\max}}(2\ell+1)\, e^{i\frac{(\ell+1/2)^2}{2\omega r}} J_0((\ell+1/2)\theta). \tag{42}$$

The relation (34) implies this sum becomes

$$|I(\theta)| = 1 + O((\omega r)^{-1}) \tag{43}$$

in the eikonal limit $\omega r \gg 1$. We present converging behavior of this sum for $\theta = 0$ case (Fig. 2).

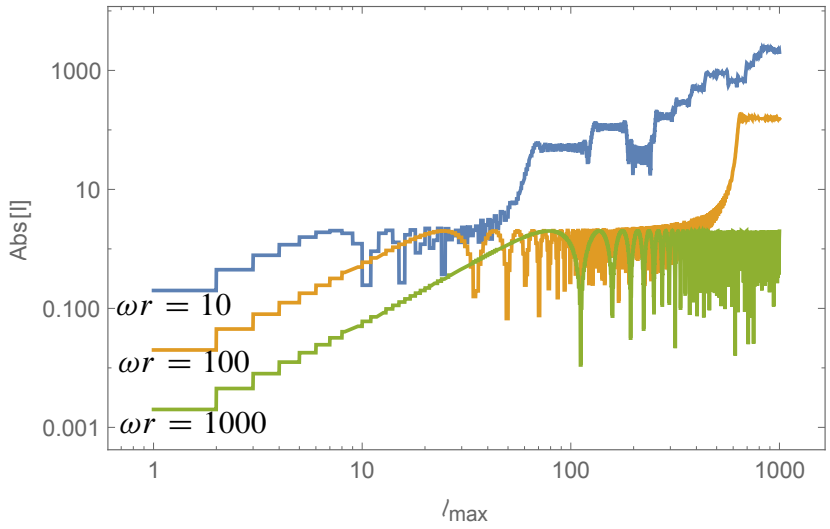

Figure 2. The partial wave sum (34) as a function of $\ell_{\max}$ for $\omega r = 10, 100, 1000$.

For $\ell_{\max} \approx \sqrt{2}\,\omega r$, we can observe the absolute value of the sum oscillates around the true value predicted by the formula (34). This oscillation is due to interference between $O((\omega r)^0)$ and $O((\omega r)^{-1})$ terms and the amplitude of the oscillation is expected to be reduced in $\omega r \gg 1$ limit. Thus we expect that the partial wave sum with $\ell_{\max} = \sqrt{2}\,\omega r$ converges in the eikonal limit.

We then checked numerically the convergence of the sum of (36) for the weak gravitational field case that is equivalent to the Coulomb scattering. We truncate the infinite sum up to the value $\ell_{\max}$ and the phase shift is evaluated by the formula (38). The convergence of the sum (39) for $\theta = 0$ is shown in Fig. 3:

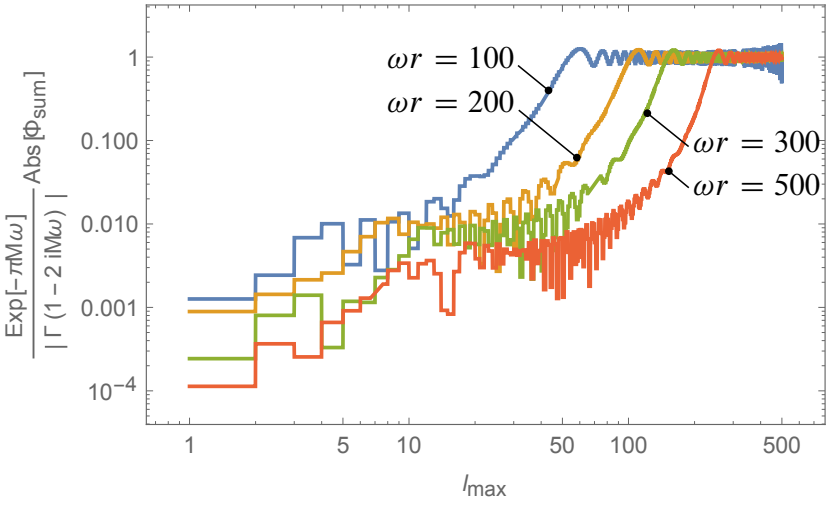

Figure 3. The convergence behavior of the sum (39) for $\theta = 0$.

We expect the absolute value of this sum becomes $e^{\pi M\omega}|\Gamma(1-2iM\omega)|$. Fig. 3 shows the sum converges to the correct value if we set $\ell_{\rm max} = \sqrt{2}\,\omega r$ and take $\omega r \gg 1$ limit. We also check the sum reproduces correct θ dependence of the scattering wave function.

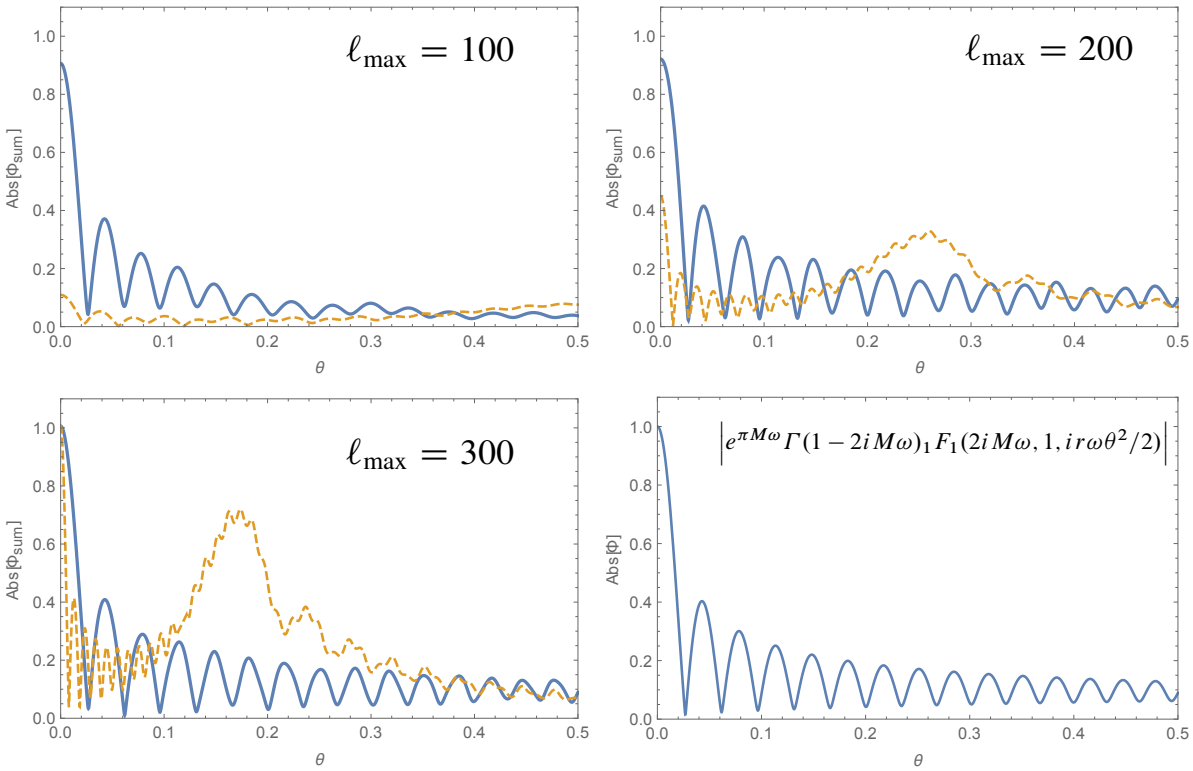

Figure 4. Behaviors of the wave function obtained by the partial wave sum up to $\ell_{\rm max}(\omega r = 200, r = 20M)$. The dotted lines are the partial wave sum without the factor $e^{i\frac{(\ell+1/2)^2}{2\omega r}}$. The last panel is behavior of the analytic function that the partial wave sum converges in the eikonal limit.

Fig. 4 shows behavior of the wave function (39) obtained by taking the partial wave sum up to $\ell_{\rm max}$ $(\omega r = 200, r = 20M)$. For $\ell_{\rm max} = 300 \sim \sqrt{2}\,\omega r$, the obtained wave function has a good agreement with the asymptotic analytic formula.

For the Schwarzschild black hole case, the WKB phase shift is evaluated by the formula (16).

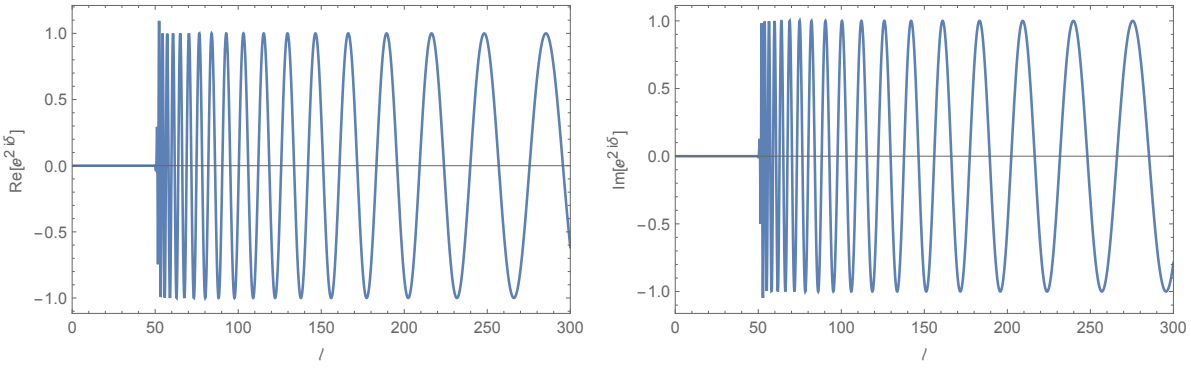

Figure 5. The WKB phase shift of the Schwarzschild black hole for $M\omega = 10$.

Fig. 5 shows appearance of the critical angular number $\ell_c \approx 51$ corresponding to the critical impact parameter $b_c = \ell_c/\omega = 3\sqrt{3}\,M$ for null rays. To make connection with the geometric optics, we plot the deflection angle introduced by the relation (19):

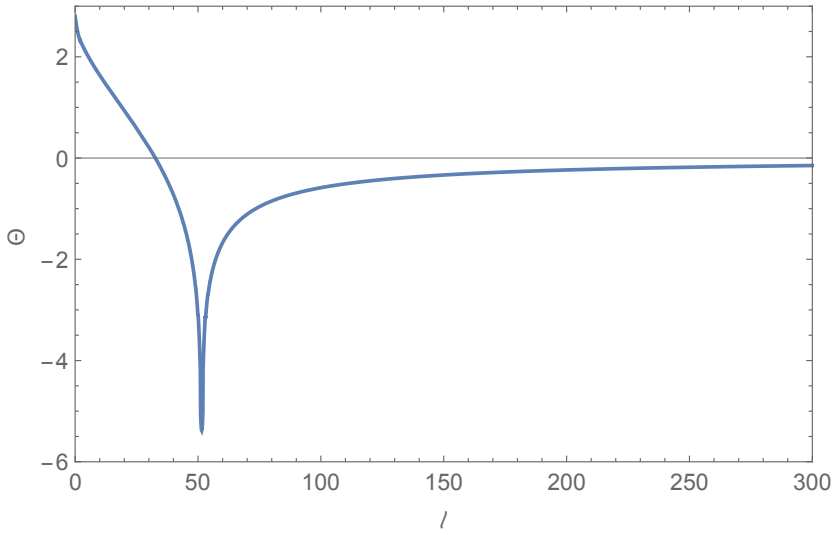

Figure 6. The deflection angle for null rays in the Schwarzschild spacetime calculated from the WKB phase shift ($M\omega = 10$). The critical angular number is $\ell_c \approx 51$.

Near the critical angular number ℓ_c, the deflection angle can have arbitrary negative values and null rays can go around the black hole arbitrary times (orbiting, Fig. 6). This feature is peculiar to black hole spacetimes that have event horizons. Fig. 7 shows the wave function calculated by taking the partial wave sum ($r = 20M$).

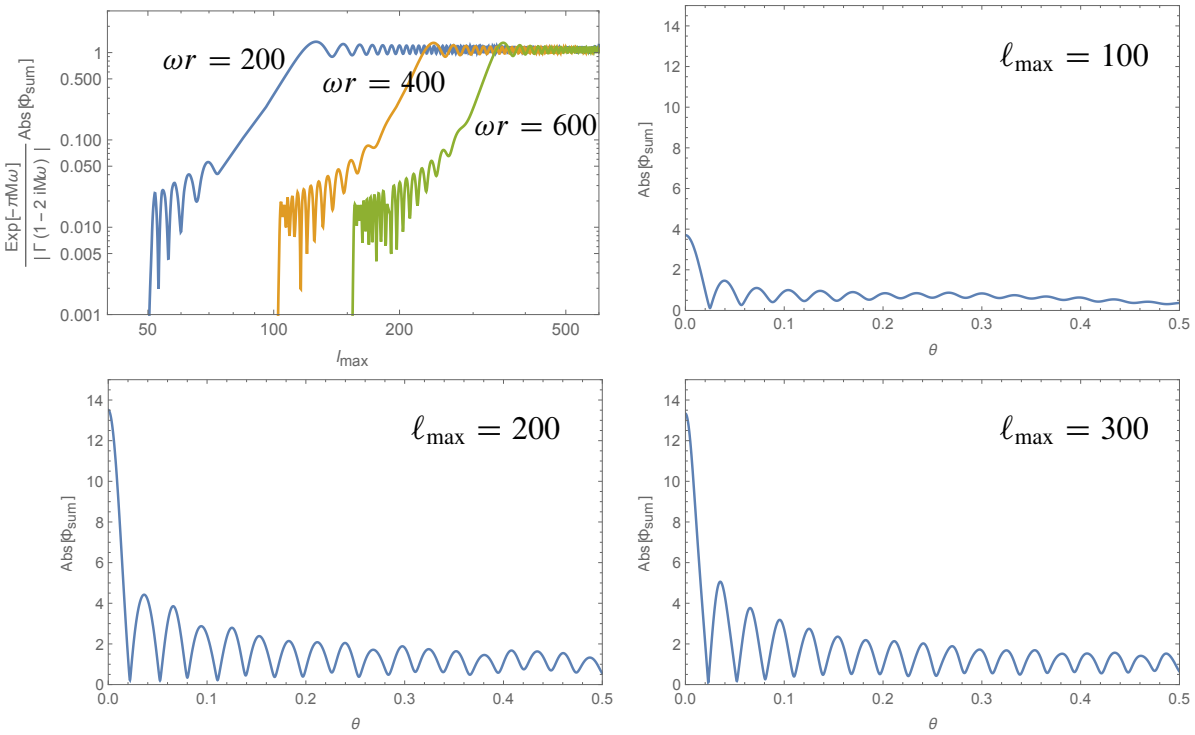

Figure 7. Behavior of the scattering wave function in the Schwarzschild spacetime obtained by the partial wave sum. The top left panel shows convergence of the wave function for $\theta = 0$ ($r = 20M$). The other panels are θ dependence of the wave function with $M\omega = 10, r = 20M$ and $\ell_{\rm max} = 100, 200, 300$.

We expect the optimal value of $\ell_{\rm max}$ for $M\omega = 10, r = 20M$ is $\sqrt{2}\,\omega r \approx 280$. Indeed, the value of the wave function for $\theta = 0$ is converging to the expected value for $\ell_{\rm max} > 200$ (the top left panel in Fig. 7).

To summarize, base on these examples investigated in this subsection, we conclude that the partial wave sum formula (36) is applicable to black hole spacetimes if we set the upper limit of the sum as $\ell_{\rm max} = \sqrt{2}\,\omega r$ and take the eikonal limit $\omega r \gg 1$. In this paper, we try to evaluate this sum analytically.

2.4. Derivation of lens equation

Applying the Poisson sum formula again to (36), the asymptotic form of the Green function is

$$\Phi \approx \frac{e^{i\omega(r_*+r_{s*})}}{4\pi i\omega r r_s}\sum_{m=-\infty}^{+\infty}\int_0^\infty d\lambda\,\lambda\, e^{i\frac{\lambda^2}{2\omega\tilde{r}}}\, e^{2i\delta_{\lambda-1/2}}\, J_0(\lambda\theta)\, e^{i2\pi m(\lambda-1/2)}, \quad \text{for} \quad \theta \ll 1. \tag{44}$$

Changing the integration variable to the semi-classical impact parameter $b = (\ell+1/2)/\omega$, the wave function (44) becomes

$$\Phi \propto \sum_{m=-\infty}^{+\infty}\int_0^\infty db\, b\, e^{i\omega\frac{b^2}{2}\left(\frac{1}{r}+\frac{1}{r_s}\right)}\, e^{2i\delta_{b\omega-1/2}}\, J_0(b\omega\theta)\, e^{i2\pi m(b\omega-1/2)}. \tag{45}$$

As the integrand is the rapidly oscillating function of b for $M\omega \gg 1$, the integral can be evaluated by the stationary phase method. Using the asymptotic form of the Bessel function‖, the stationary phase condition for the integrand yields

$$b\left(\frac{1}{r}+\frac{1}{r_s}\right) = -\Theta(b) - 2\pi m \pm \theta, \quad \Theta(\lambda) \equiv 2\frac{d\delta_\lambda}{d\lambda}. \tag{46}$$

$\Theta(b)$ is the deflection function which coincides with the classical deflection angle (11). This is the lens equation for the black hole spacetime. For a given position of the source and the observer (r, r_s, θ), this equation provides the impact parameter b and determines the trajectory of null rays connecting the source and the observer. The integer m has the meaning of the winding number for null rays orbiting around the black hole. The geometric interpretation of this equation is shown in Fig. 8:

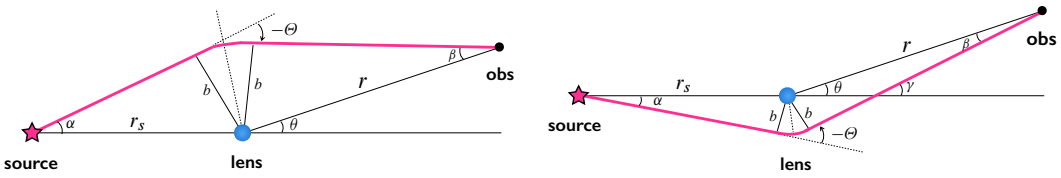

Figure 8. Configuration of the gravitational lensing in the geometric optics. Angles in the figure satisfy $\alpha+\beta = -\Theta+\theta$ in the left panel and $\alpha+\beta = -\Theta-\theta$ in the right panel.

Angles α, β satisfies the relation

$$\alpha + \beta = -\Theta \pm \theta, \tag{47}$$

where $+$ sign corresponds to the left panel and $-$ sign corresponds to the right panel in Fig. 8. Using $\alpha \approx \frac{b}{r_s} \ll 1$ and $\beta \approx \frac{b}{r} \ll 1$, we obtain

$$b\frac{r_s + r}{r r_s} = -\Theta \pm \theta. \tag{48}$$

This is the lens equation (46) with $m = 0$. For $-\Theta > 2\pi$, the null ray goes around the black hole more than one times (orbiting). In such a case, the winding number m is defined so as the condition $0 < -\Theta - 2\pi m < 2\pi$ is satisfied.

3. S-matrix and Regge poles for wave scattering by black holes

For the partial waves with impact parameter $b \sim 3\sqrt{3}M$, the scattering occurs in the vicinity of the peak of the effective potential (Fig. 9).

‖

$$J_0(x) \sim \sqrt{\frac{2}{\pi x}}\cos(x - \pi/4) \quad \text{for} \quad |x| \gg 1.$$

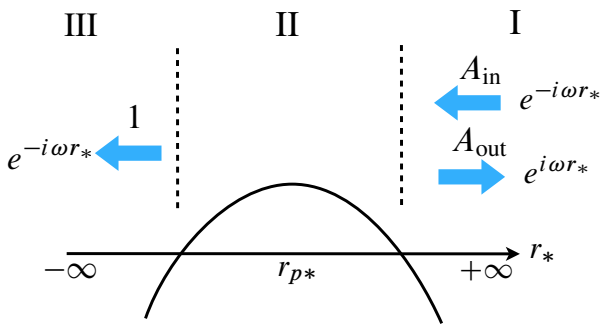

Figure 9. The effective potential $Q(x)$ around the unstable circular orbit r_p. The quasi-normal mode satisfies $A_{\rm out}/A_{\rm in} = \infty$.

Using the result of the asymptotic matching of the WKB wave function around the peak, the S-matrix $S_\ell \equiv e^{2i\delta_\ell}$ is obtained as

$$S_\ell = -(-)^\ell \frac{A_{\rm out}}{A_{\rm in}} = -(-)^\ell \frac{e^{i\pi\nu}}{\sqrt{2\pi}} \left(\nu + \frac{1}{2}\right)^{\nu+1/2} e^{-(\nu+1/2)} \Gamma(-\nu), \tag{49}$$

where ν is determined by the relation [25]

$$\nu + \frac{1}{2} = i\frac{Q_0}{\sqrt{2Q_0''}} \approx \frac{27M^2\omega^2 - \ell^2}{2\,\ell}. \tag{50}$$

The peak of the potential for the Schwarzschild case is at $r_p = 3M$ and

$$Q_0 = Q(r_p), \quad Q_0'' = \partial_{r_*}^2 Q\big|_{r=r_p}. \tag{51}$$

Absolute value of S_ℓ represents the reflection rate of incident waves. As the black hole absorbs waves, the phase shift acquires the imaginary part and the reflection rate becomes smaller than unity for small impact parameters. Indeed,

$$|S_\ell|^2 = e^{-2\delta_I} = \frac{1}{1 + \exp\left(-\pi\frac{\ell^2 - 27(M\omega)^2}{2\ell}\right)} \approx \frac{1}{1 + \exp\left(-\pi(\ell - \ell_c)\right)}, \tag{52}$$

where $\ell_c = 3\sqrt{3}M\omega$ is the critical angular momentum. The waves with $\ell < \ell_c$ are absorbed by the black hole. $b_c = \ell_c/\omega = 3\sqrt{3}M$ is the critical impact parameter (Fig. 10).

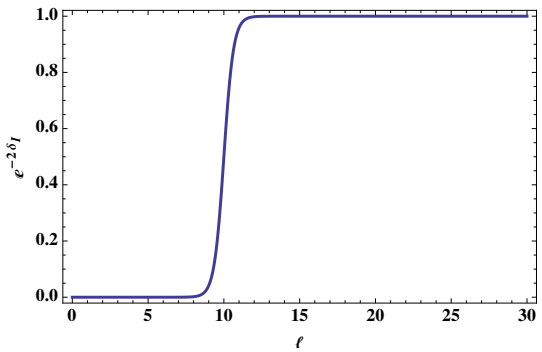

Figure 10. The reflection rate for $\ell_c = 10$.

The S-matrix (49) has poles in the complex ℓ plane of which location is determined by poles of the Gamma function $\Gamma(-\nu), \nu = n,\ n = 0, 1, 2, \cdots$. That is, poles of the S-matrix in the complex ℓ plane are ¶

$$\ell_n \approx \ell_c + i\left(n + \frac{1}{2}\right), \quad \ell_c = 3\sqrt{3}M\omega, \quad n = 0, 1, 2, \cdots \tag{53}$$

These are Regge poles [22]. In the vicinity of the nth pole ℓ_n, the S-matrix is

$$S_\ell \approx \frac{\gamma_n}{\ell - \ell_n}, \quad \gamma_n = (-)^{\ell_c}\frac{i}{\sqrt{2\pi}}\left(\frac{\ell_n}{\ell_c}\right)\left(n + \frac{1}{2}\right)^{n+1/2} e^{-(n+1/2)}\frac{1}{n!}. \tag{54}$$

For $n \gg 1$, $n! \approx \sqrt{2\pi n}\, e^{-n} n^n$, $(1 + 1/(2n))^{n+1/2} \approx e^{1/2}$, hence the residue γ_n is

$$\gamma_n \approx (-)^{\ell_c}\frac{i}{2\pi}\frac{\ell_n}{\ell_c}. \tag{55}$$

4. Evaluation of scattering wave

The formula of the Green function (44) is decomposed to $m = 0$ and $m \neq 0$ parts:

$$\Phi = \frac{e^{i\omega(r_* + r_{s*})}}{4\pi i\omega r r_s}\left[\int_0^\infty d\lambda\, \lambda\, e^{i\frac{\lambda^2}{2\omega\tilde{r}}}\, e^{2i\delta_{\lambda-1/2}}\, J_0(\lambda\theta) + \sum_{m\neq 0}\int_0^\infty d\lambda\, \lambda\, e^{i\frac{\lambda^2}{2\omega\tilde{r}}}\, e^{2i\delta_{\lambda-1/2}}\, J_0(\lambda\theta)\, e^{i2\pi m(\lambda-1/2)}\right]. \tag{56}$$

As we have discussed in Sec. 2.3, the integer m is the winding number for null rays orbiting around the black hole. Hence the first integral term represents contribution of rays which directly reach the observer (direct part). By identifying the phase shift as the lens potential of the gravitational lensing, the direct part reproduces the Kirchoff-Fresnel diffraction formula for the gravitational lensing [10]. On the other hand, the second integral term represents the contribution of rays go around the black hole (winding part). We evaluate these two parts separately.

4.1. Winding part : contribution of Regge poles

As the S-matrix has poles in the complex ℓ plane, the integral of the second term in (56) can be evaluated by applying Cauchy's theorem. We use the contour shown in Fig. 11. We first show that the integral along the circle $|\lambda| = R$ vanishes as $R \to \infty$. Introducing a new integration variable $y^2 = -i\lambda^2/(2\omega\tilde{r})$,+

$$\int_{|\lambda|=R} d\lambda\lambda e^{i\frac{\lambda^2}{2\omega\tilde{r}}} e^{2i\delta_{\lambda-1/2}} J_0(\lambda\theta) e^{i2\pi m(\lambda-1/2)}$$

¶ The quasi-normal frequency is given by treating ℓ as real:

$$\omega_n = \frac{1}{3\sqrt{3}M} - \frac{i}{3\sqrt{3}M}\left(n + \frac{1}{2}\right).$$

+ To show that the integral along the circle vanishes, we use the formula

$$e^{-y^2} = \frac{1}{\sqrt{\pi}}\int_{-\infty}^{+\infty} dk\, e^{-k^2 + 2iky}.$$

$$= \frac{1}{\sqrt{\pi}} \int_{-\infty}^{+\infty} dk e^{-k^2} \int_{|\lambda|=R} d\lambda\lambda \exp\left[\left(\frac{2ke^{i\alpha}}{\sqrt{2\omega\tilde{r}}} + i2\pi m\right)\lambda\right] e^{2i\delta_{\lambda-1/2}} J_0(\lambda\theta) e^{-i\pi m},$$

where we choose $\alpha = 5\pi/4$ for $\mathrm{Im}(\lambda) > 0$ and $\alpha = -\pi/4$ for $\mathrm{Im}(\lambda) < 0$ for convergence of the integral. Hence, as $R \to \infty$, the integral becomes zero.

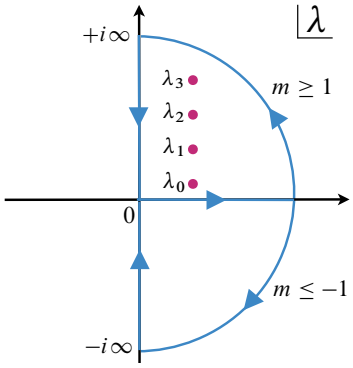

Figure 11. Poles of the S-matrix are situated in the first quadrant of the complex λ plane.

Thus the second integral in (56) has contributions from poles and the integral along the imaginary axis.

$$\sum_{m=1}^{\infty}\sum_{n=0}^{\infty} \ell_n e^{i\frac{\ell_n^2}{2\omega\tilde{r}}} (2\pi i\gamma_n) J_0(\ell_n\theta) e^{i2\pi m(\ell_n - 1/2)} + \sum_{m=1}^{\infty} \int_0^{+i\infty} d\lambda + \sum_{m=-1}^{-\infty} \int_0^{-i\infty} d\lambda. \quad (57)$$

The integral along the positive imaginary axis is

$$\begin{aligned}\sum_{m=1}^{\infty} \int_0^{+i\infty} &\approx \int_0^{+i\infty} d\lambda\lambda \frac{i}{2} \frac{e^{i\pi(\lambda-1/2)}}{\sin(\pi(\lambda-1/2))} e^{i\frac{\lambda^2}{2\omega\tilde{r}}} e^{2i\delta_{\lambda-1/2}} J_0(\lambda\theta) \\ &= -\frac{i}{2} \int_0^{\infty} d\tilde{\lambda}\,\tilde{\lambda} \frac{(-i)e^{-\pi\tilde{\lambda}}}{1/2(e^{-\pi\tilde{\lambda}} + e^{\pi\tilde{\lambda}})} e^{-i\frac{\tilde{\lambda}^2}{2\omega\tilde{r}}} e^{2i\delta_{-i\tilde{\lambda}-1/2}} J_0(i\tilde{\lambda}\theta) \\ &= O(\omega^0), \end{aligned} \quad (58)$$

and yields higher order contribution in the eikonal limit because the first integral in (56) gives $O(\omega)$ contribution. The contribution of the integral along the negative imaginary axis is also $O(\omega^0)$. We ignore these terms in our treatment. Thus, the wave function (56) becomes

$$\Phi \approx \frac{e^{i\omega(r_* + r_{s*})}}{4\pi i\omega r r_s} \left[\int_0^{\infty} d\lambda\,\lambda\, e^{i\frac{\lambda^2}{2\omega\tilde{r}}} e^{2i\delta_{\lambda-1/2}} J_0(\lambda\theta) + 2\pi i \sum_{n=0}^{\infty} \ell_n \gamma_n e^{i\frac{\ell_n^2}{2\omega\tilde{r}}} J_0(\ell_n\theta) f(\ell_n)\right], \quad (59)$$

where

$$f(\ell_n) \equiv \sum_{m=1}^{\infty} e^{2i\pi m(\ell_n - 1/2)} = -\frac{e^{2i\pi\ell_n}}{e^{2i\pi\ell_n} + 1}. \quad (60)$$

The sum over n can be evaluated by applying the Euler-Maclaurin formula and keeping the contribution of the leading order in the eikonal limit:

$$
\begin{aligned}
&2i\pi \sum_{n=0}^{\infty} \ell_n \, \gamma_n \, e^{i\frac{\ell_n^2}{2\omega\tilde{r}}} \, J_0(\ell_n \theta) \, f(\ell_n) \\
&\quad \approx -\frac{e^{i\pi\ell_c}}{\ell_c} \int_0^{\infty} dn \left(\ell_c + \frac{i}{2} + in\right)^2 e^{\frac{i}{2\omega\tilde{r}}\left(\ell_c + \frac{i}{2} + in\right)^2} J_0\left[\left(\ell_c + \frac{i}{2} + in\right)\theta\right] f\left(\ell_c + \frac{i}{2} + in\right) \\
&\quad \approx \sqrt{\frac{\pi}{2}} \, e^{-\pi - i\pi/4 + i3\pi\ell_c} e^{\frac{i\ell_c^2}{2\omega\tilde{r}}} \, \ell_c \sqrt{\omega\tilde{r}} \, J_0(\ell_c\theta) + O\left(\frac{1}{\sqrt{\omega\tilde{r}}}\right). \qquad (61)
\end{aligned}
$$

We have used

$$
f\left(\ell_c + \frac{i}{2}\right) \approx -e^{2i\pi\ell_c} e^{-\pi}. \qquad (62)
$$

After all, we obtain

$$
\Phi \approx \frac{e^{i\omega(r_* + r_{s*})}}{4\pi i\omega r r_s} \left[\int_0^{\infty} d\lambda \, \lambda \, e^{i\frac{\lambda^2}{2\omega\tilde{r}}} \, e^{2i\delta_\lambda} J_0(\lambda\theta) + \sqrt{\frac{\pi}{2}} \, e^{-\pi - i\pi/4 + i3\pi\ell_c} e^{\frac{i\ell_c^2}{2\omega\tilde{r}}} \, \ell_c \sqrt{\omega\tilde{r}} J_0(\ell_c\theta)\right]. \quad (63)
$$

4.2. Direct part and total wave function

We evaluate this term assuming that impact parameters of corresponding null rays are not so small and gravitational field can be approximated by the Newtonian weak field. Within such an assumption, the phase shift can be approximated by that of the weak field form (38) and the direct part can be obtained as (39). Therefore, the formula for the total scattering wave is summarized as follows:

$$
\Phi \approx \frac{e^{i\omega(r_* + r_{s*})}}{4\pi(r + r_s)} \Big[c_1 J_0(b_E\omega\theta) + c_2 J_0(b_c\omega\theta)\Big], \quad \text{for} \quad \theta \ll 1, \qquad (64)
$$

$$
c_1 = e^{-i2M\omega \ln 2M\omega} e^{\pi M\omega} \Gamma(1 - i2M\omega) e^{-\frac{i}{4}\omega\tilde{r}\theta^2}, \quad c_2 = -i\sqrt{\frac{\pi}{2\omega\tilde{r}}} \, \ell_c \, e^{-\pi} \, e^{i\left(\frac{\ell_c^2}{2\omega\tilde{r}} + 3\pi\ell_c - \frac{\pi}{4}\right)},
$$

where $b_E = \sqrt{4M\tilde{r}}$ is the Einstein radius and $b_c = 3\sqrt{3}M$ is the critical impact parameter for null rays. This formula is applicable for $r, r_s \gg 2M$ and $M\omega \gg 1$. Let us assume that the point source is near the black hole and the observer is sufficiently far from the black hole ($r \gg r_s$). Then $\tilde{r} \approx r_s$. Of course the location of the source must be far from the black hole to apply (64), we dare to consider such a situation to investigate the wave optical image and the interference effect by the black hole. As the impact parameters for the direct rays must be larger than those of the winding rays, we must require $b_E > b_c$ which constrains the distance of the point source from the black hole in our approximation:

$$
r_s > \frac{27}{4}M \equiv r_c \sim 6.8M. \qquad (65)
$$

The ratio of two coefficients is

$$
\frac{|c_2|}{|c_1|} = \frac{3}{2}\sqrt{\frac{3M}{r_s}} \times e^{-\pi} = e^{-\pi}\left(\frac{r_s}{r_c}\right)^{-1/2} \approx 0.043 \times \left(\frac{r_s}{6.8M}\right)^{-1/2}. \qquad (66)
$$

In the geometrical optics, it is known that the intensity of the winding ray reduces to the factor $e^{-2\pi} \approx 0.0019$ compared to the direct ray [5]. In terms of the amplitude of the wave, this value corresponds to $e^{-\pi} \approx 0.043$ and is consistent with the obtained value $|c_2|/|c_1|$ in the eikonal limit of the scattering wave function.

5. Applications

As applications of the analytic formula (64) of the scattering wave, let us consider images of the black hole and the interference effect in the frequency domain.

5.1. Wave optical image of black holes

Using the scattering wave function (64), we can reconstruct wave optical images of black holes illuminated by a point source [9]. As the imaging system, we consider a detector with a convex lens which transforms the interference fringe to the image (Fig. 12).

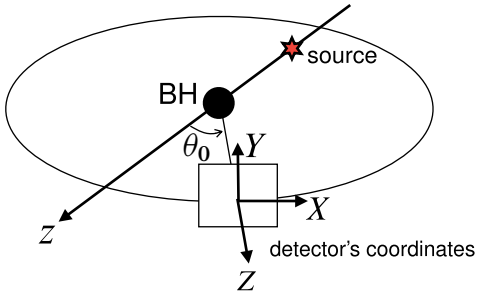

Figure 12. The configuration of the imaging system with a convex lens.

The location of the lens of the detector is $Z = 0$ in the detector's coordinates and the wave function just in front of the lens is $\Phi(X, Y, 0)$. Using the Fresnel-Kirchoff diffraction formula [26], the wave on the detector's focal plane $Z = f$ is given by

$$\Phi_I(X_I, Y_I) \propto \int_{X^2+Y^2 \leq a^2} dX dY\, \Phi(X, Y, 0)\, e^{-i\omega \frac{X^2+Y^2}{2f}} \times \frac{e^{i\omega\ell}}{\ell} \tag{67}$$

where X_I, Y_I are coordinates on the focal plane, a is a radius of the lens and ℓ is the path length between a point on the lens plane and a point on the focal plane. The function $e^{-i\omega \frac{X^2+Y^2}{2f}}$ in (67) represents the action of the convex lens which transform incident plane waves to spherical waves focusing at the focal point. Assuming that the focal length is sufficiently larger than the radius of the lens,

$$\ell = \sqrt{(X - X_I)^2 + (Y - Y_I)^2 + f^2} \approx f + \frac{(X - X_I)^2 + (Y - Y_I)^2}{2f}, \tag{68}$$

and we obtain

$$\Phi_I(X_I, Y_I) \propto \int_{X^2+Y^2 \leq a^2} dX dY\, \Phi(X, Y, 0)\, e^{-i\frac{\omega}{f}(X_I X + Y_I Y)}. \tag{69}$$

Thus the wave function Φ_I on the focal plane is the Fourier transformation of the wave function Φ. The relation between the world coordinates (x, y, z) and the detector's coordinates (X, Y, Z) is

$$\begin{aligned} x &= r\sin\theta\cos\phi = X\cos\theta_0 - Z\sin\theta_0, \\ y &= r\sin\theta\sin\phi = Y, \\ z &= r\cos\theta = X\sin\theta_0 + Z\cos\theta_0, \quad X^2+Y^2+Z^2 = r^2. \end{aligned} \tag{70}$$

It is possible to obtain $\cos\theta$ as a function of X, Y:

$$\cos\theta = \left(\frac{X}{r}\right)\sin\theta_0 + \sqrt{1-\left(\frac{X}{r}\right)^2 - \left(\frac{Y}{r}\right)^2}\cos\theta_0. \tag{71}$$

Fig. 13 shows an example of images of the Schwarzschild black hole illuminated by a point source. Images are obtained by drawing $|\Phi_I|$ which is the amplitude of the Fourier transformation of Φ.

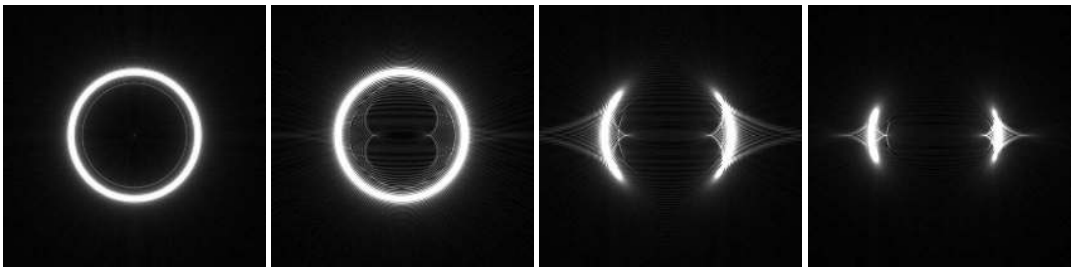

Figure 13. Images of the black hole for different viewing angles $\theta_0 = 0.0, 0.02, 0.05, 0.09$ (from the left to the right panels). Parameters are $r_s = 10M, r = \infty$. $M\omega = 800$ and $a = 0.03$.

In our previous paper [9], we numerically solved the Helmholtz equation in the Schwarzschild spacetime and images of the black hole are reconstructed using the obtained wave function. Due to limited resolution of the numerical calculation, it was difficult to perform simulation with high frequency waves corresponding to the eikonal limit and it was hard to resolve the fine structure of black hole images. In the present analysis, as we have obtained the analytic form of the scattering waves, it is possible to acquire images using high frequency waves. In Fig. 13, we can observe a bright outer ring which corresponds to the Einstein ring by direct rays and a thin inner ring which corresponds to the rim of the black hole shadow (photon ring). It was not easy to recognize this structure of the black hole images in our previous paper [9].

5.2. Interference effect in wave scattering by black holes

We can examine the interference effect in the frequency domain using (64); that is caused by the interference between the direct rays and the winding rays. For $b_E\omega\theta, b_c\omega\theta \gg 1$, using the asymptotic form of the Bessel function, the scattering wave (64) can be written as

$$\Phi \sim d_1\cos(b_E\omega\theta_0) + d_2\cos(b_c\omega\theta_0), \tag{72}$$

where d_1, d_2 represent numerical factors independent of ω with their ratio

$$\frac{|d_2|}{|d_1|} = e^{-\pi}\left(\frac{r_s}{r_c}\right)^{-1/2}. \tag{73}$$

After averaging the amplitude of the wave over rapidly oscillating frequency scale $\sim 1/(M\theta_0)$, the power spectrum is

$$I(\omega) = |\Phi|^2 \sim \frac{|d_1|^2}{2} + \frac{|d_2|^2}{2} + \frac{d_1 d_2^* + d_1^* d_2}{2}\cos\left[(b_E - b_c)\omega\theta_0\right]. \tag{74}$$

The first term and the second term represent the intensity of the direct wave and the winding wave, respectively. The third term represents the interference between the direct wave and the winding wave. For the point source at $r_s \sim 7M$, the impact parameters for the direct rays and the winding rays become nearly equal and the interference term results in the "beat" in the frequency domain. The modulation due to the interference appears in the power spectrum (Fig. 14).

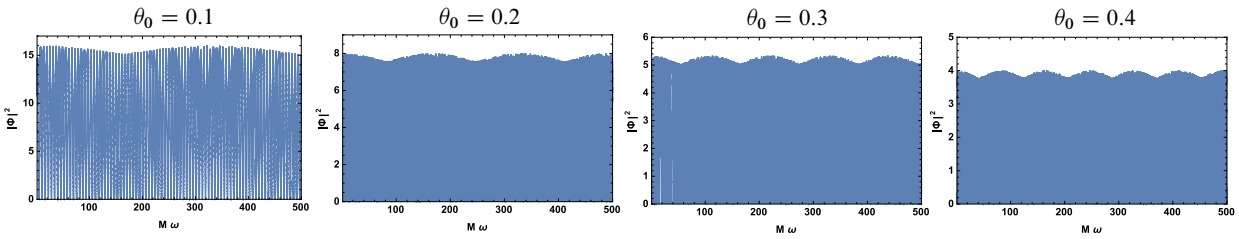

Figure 14. The power spectrum of the scattering wave with $r_s = 7M$. The amplitude of the modulation is $\Delta I/I \sim 0.1$. The period of the modulation depends on the viewing angle θ_0.

The period of the modulation in the power spectrum is

$$M\Delta\omega = \frac{2\pi}{\theta_0}\frac{1}{3\sqrt{3}}\left(\sqrt{\frac{r_s}{27M/4}} - 1\right)^{-1}. \tag{75}$$

As the typical value for the viewing angle θ_0, if the Einstein angle $\theta_E = \sqrt{4M/r_s}$ is assumed, we obtain

$$M\Delta\omega = \frac{\pi}{2 - 3\sqrt{\frac{3M}{r_s}}}, \quad r_s > \frac{27M}{4}. \tag{76}$$

For $r_s \sim r_c$, the visibility of the modulation is

$$V \equiv \frac{I_{\max} - I_{\min}}{I_{\max} + I_{\min}} = \frac{d_1 d_2^* + d_1^* d_2}{|d_1|^2 + |d_2|^2} \sim 2e^{-\pi} \sim 0.08. \tag{77}$$

This value is not so small and we may have the possibility to detect this interference effect observationally, which means direct verification of the black hole spacetime.

	galactic core BH	intermediate mass BH	stellar mass BH
mass	$10^6 M_\odot$	$10^3 M_\odot$	$10 M_\odot$
$\Delta\omega$	40Hz	40kHz	4MHz

Table 1. The typical frequency of the modulation in the power spectrum.

Table I shows the frequencies $\Delta\omega$ for black holes with different masses. For intermediate mass black holes and stellar mass black holes, the modulation in the power spectrum is expected to be detectable using sub-mm radio telescopes with suitable band width and the frequency resolution.

6. Summary

We investigated the wave optics in the Schwarzschild spacetime following the standard treatment of the wave scattering problem and evaluated the Green function for the stationary monochromatic point source in the eikonal limit. To make the partial wave sum of the scattering wave converge, we retain the next to leading order contribution in the phase of the partial waves for large r. Effect of the orbiting scattering is taken into account as the contribution of Regge poles to the scattering wave. The wave optical images of the black hole are obtained and the interference effect in the frequency domain is discussed.

As the straightforward extension of the analysis performed in this paper, the formulation of the wave optics in the Kerr spacetime is now on going. We expect that the effect associated with the black hole spin such as the superradiance adds new features to the scattered wave. We will report on this subject in our forthcoming paper.

Acknowledgments

The authors thank the anonymous referee who pointed out the importance of convergence of the partial wave sum. This work was supported in part by the JSPS KAKENHI Grant Number 15K05073. The authors also thanks all member of "black hole horizon project meeting" in which the preliminary version of this paper was presented.

References

[1] B. Mashhoon, "Stability of charged rotating black holes in the eikonal approximation", *Phys. Rev. D* **31**, (1985) 290–293.

[2] V. Cardoso, A. Miranda, E. Berti, H. Witek, and V. Zanchin, "Geodesic stability, Lyapunov exponents, and quasinormal modes", *Phys. Rev. D* **79**, (2009) 064016.

[3] H. Yang, D. a. Nichols, F. Zhang, A. Zimmerman, Z. Zhang, and Y. Chen, "Quasinormal-mode spectrum of Kerr black holes and its geometric interpretation", *Phys. Rev. D* **86**, (2012) 104006.

[4] H. Yang, F. Zhang, A. Zimmerman, and Y. Chen, "Scalar Green function of the Kerr spacetime", *Phys. Rev. D* **89**, (2014) 064014.

[5] V. P. Frolov and I. Novikov, *Black Hole Physics* (Klewer Academic Publisher, Dordrecht, 1998).

[6] H. Falcke, F. Melia, and E. Agol, "VIEWING THE SHADOW OF THE BLACK HOLE AT THE GALACTIC CENTER", *Astrophys. J. Lett.* **528**, (2000) 13–16.

[7] R. Takahashi, "Shapes and Positions of Black Hole Shadows in Accretion Disks and Spin Parameters of Black Holes", *Astrophys. J.* **611**, (2004) 996–1004.

[8] Y. Nambu, "Wave Optics and Image Formation in Gravitational Lensing", *Int. J. Astron. Astrophys.* **03**, (2013) 1–7.

[9] K.-i. Kanai and Y. Nambu, "Viewing black holes by waves", *Class. Quantum Gravity* **30**, (2013) 175002.
[10] P. Schneider, J. Ehlers, and E. E. Falco, *Gravitational lenses* (Springer-Verlag, Berlin, 1992).
[11] S. Deguchi and W. D. Watson, "Diffraction in gravitational lensing for compact objects of low mass", *Astrophys. J.* **307**, (1986) 30.
[12] T. T. Nakamura and S. Deguchi, "Wave Optics in Gravitational Lensing", *Prog. Theor. Phys. Suppl.* **133**, (1999) 137–153.
[13] C. Baraldo, A. Hosoya, and T. Nakamura, "Gravitationally induced interference of gravitational waves by a rotating massive object", *Phys. Rev. D* **59**, (1999) 083001.
[14] A. Gould, "Femtolensing of gamma-ray bursters", *Astrophys. J.* **386**, (1992) L5.
[15] N. Andersson and B. Jensen, "Scattering by black holes", *arXiv gr-qc/0011025.*
[16] K. Glampedakis and N. Andersson, "Scattering of scalar waves by rotating black holes", *Class. Quantum Gravity* **18**, (2001) 1939–1966.
[17] Y. Décanini, A. Folacci and B. Jensen "Complex angular momentum in black hole physics and quasinormal modes", *Phys. Rev. D* **67**, (2003) 124017.
[18] Y. Décanini and A. Folacci, "Regge poles of the Schwarzschild black hole: A WKB approach", *Phys. Rev. D* **81**, (2010) 024031.
[19] Y. Décanini, G. Esposito-Farèse, and A. Folacci, "Universality of high-energy absorption cross sections for black holes", *Phys. Rev. D* **83**, (2011) 044032.
[20] K. W. Ford and J. A. Wheeler, "Semiclassical description of scattering", *Ann. Phys.* **7**, (1959) 259–286.
[21] M. V. Berry, "Uniform approximations for glory scattering and diffraction peaks", *J. Phys. B (At. Mol. Phys.)* **2**, (1969) 381–392.
[22] R. G. Newton, *Scattering Theory of Waves and Particles* (Dover Publications, Inc., New York, 1982).
[23] N. Andersson, "Complex angular momenta and the black-hole glory", *Class. Quantum Gravity* **11**, (1994) 3003–3012.
[24] J. Futterman, F. Handler, and R. Matzner, *Scattering from black holes* (Cambridge University Press, New York, 1987).
[25] S. Iyer and C. Will, "Black-hole normal modes: A WKB approach. I. Foundations and application of a higher-order WKB analysis of potential-barrier scattering", *Phys. Rev. D* **35**, (1987) 3621–3631.
[26] K. Sharma, *Optics: principles and applications* (Academic Press, Tokyo, 2006).